JNPS 10 (2): 59- 68 (2024)
ISSN: 2392-473X(Print), 2738-9537 (Online)
Research Article *©Nepal Physical Society*
doi.org/10.3126/jnphyssoc.v10i2.79492

The Structural and Binding Activity of Tenofovir from Density Functional Theory

Manoj Kumar Chaudhary[1], Sushil Poudel[1*], Jagadish Shahi[1], Puskar Raj Sharma[1]
[1]Department of Physics, Tribhuvan University, Amrit Campus, Institute of Science and Technology, Kathmandu 44600, Nepal
**Corresponding author: poudelsushil75@gmail.com (S. Poudel)*

Submitted: December 15, 2024; **Revised:** May 25, 2025; Acceped: June 01, 2025

Abstract

The structural and vibrational characteristics of tenofovir have been calculated from density functional theory (DFT) by implementing the theory B3LYP/3-21G basis set. Based on Fourier Transform infrared (FT-IR), Fourier Transform Raman (FT-Raman), the spectroscopic characteristics of the compound under investigation have been closely examined. With the use of molecular electrostatic potential (MEP) surface analysis and local reactivity descriptors, the charge distribution around the molecular system has been examined in order to distinguish the nucleophilic and electrophilic regions. The red regions in MEP map across P1-O5 and O4-H signify nucleophilic sites and the blue color across amine group indicate the electrophilic centers. Additionally, global reactivity descriptors based on the energy of highest occupied molecular orbital (HOMO) and lowest unoccupied molecular orbital (LUMO) have been used in predicting the molecule's chemical reactivity. The HOMO-LUMO gap is found to be 5.58 eV. The structural stability of compound based on donor and acceptor Lewis type orbital from natural bond orbital (NBO) analysis give the information that the transition LP(1) C15→ π(N9-C18) has major role for stability of compound and gives the stabilization energy 114.43 kcal/mol. Similarly, structural analysis and quantum chemical computation techniques have been used to study the fundamental chemical reactive regions of the tenofovir molecule. The highest value of Fukui function (FF) f_k^- across C16 is (0.1467) which is prone to nucleophilic center in the compound and the highest FF f_k^+ (~ 0.1787) across N10 predict the electrophilic site in the compound. These findings are essential for further research using vibrational spectroscopy on drug-target interactions.*

Keywords: DFT, FT-IR, FT-Raman, HOMO-LUMO, MEP, Tenofovir

1. Introduction

The respective molecular weight and molecular formula of tenofovir are 287.21 g/mol and $C_9H_{14}N_5O_4P$. The IUPAC name of tenofovir is [(2R)-1-(6-aminopurin-9-yl) propan-2- yl]oxymethylphosphonic acid [1]. Tenofovir disoproxil fumarate (DF) is highly effective for the suppression of hepatitis B virus (HBV) in chronically infected adults. Despite recent vaccination campaigns' success, chronic hepatitis B (CHB) remains a significant global healthcare issue and the root of severe liver disease [2]. Tenofovir DF is an oral pro-drug of tenofovir, a nucleotide (nucleoside monophosphate) analogue that is active against retroviruses such as HIV-1, HIV-2, and

hepadna viruses, when tenofovir DF is absorbed then it is quickly transformed into tenofovir [4,5]. Tenofovir is not a substrate, inducer, or inhibitor of human cytochrome P450 enzymes, either in vitro or in vivo. Tenofovir DF has been studied in conjunction with different antiviral and concomitant medications routinely used in HIV-1 infected individuals. With the exception of didanosine and atazanavir, which require dosage changes, there have been no clinically significant drug interactions with tenofovir DF [6].

The literature review reveals that the many biological and clinical research of tenofovir have been conducted by many research groups. But, the geometry optimization, reactive sites as well as spectroscopic behavior of tenofovir have not been conducted so far. In this manuscript we have examined the optimized parameters: bond length and bond angle, natural bond orbital (NBO) analysis, spectroscopic behavior (FT-IR and FT-Raman), MEP analysis, global and local reactivity activity of the investigated compound.

2. Materials and Methods

The title compound was computationally evaluated using the Gaussian 09 software program [7]. The optimization was done using the default settings of the Gaussian09 application package. The title compound is optimized using DFT with functional B3LYP [8,9] and the 3-21G basis set [10-12]. The hyperconjucative interaction energy for the stability of molecular system has been calculated from NBO 3.1 program added in Gaussian 09 program. The MEP, HOMO-LUMO, and Mulliken charges were computed using the same level of theory as optimization. GaussView 05 software was used to visualize charge distribution in molecules, including MEP, HOMO, and LUMO [13,14].

3. Results and Discussion

3.1 Geometry Optimization

The optimized molecular structure of tenofovir with the labeling of atoms is shown in Figure 1.

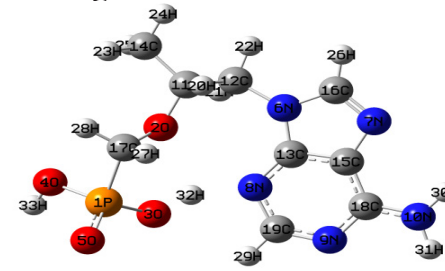

Figure 1: The optimized structure of tenofovir from B3LYP/3-21G.

The ground state energy of tenofovir was calculated as -7.91×10^{5} kcal/mol from B3LYP/3-21G. Optimized bond lengths and bond angles of tenofovir calculated from same level of theory. It is observed that the minimum bond length is 0.99 Å across O4-H33 whereas the maximum bond length is obtained as 1.87 Å across P1-C17. This respective least and highest value of bond length is due to the intermolecular hydrogen bond with surrounding species. This is justified by MEP surface analysis. Similarly the maximum and minimum bond angles are observed across 131.16 ° and 96.48 ° across N6-C13-N8 and O4-P1-C17 respectively. This is due to intermolecular hydrogen bonding with neighboring molecules in crystal packing.

But our research is for single molecule in gaseous state.

3.2Frontier Molecular Orbital (FMO's) Analysis

The pictorial representation of the frontier molecular orbitals (FMOs) as depicted in Figure 2. In general highest occupied molecular orbital (HOMO) and the lowest unoccupied molecular orbital (LUMO) are called FMOs, and these orbitals have crucial role to evaluate the reactivity and the stability of the molecules [15]. More importantly, the HOMO has tendency to donate the electrons and the LUMO has tendency to accept the electrons [16]. A molecule having a high HOMO - LUMO energy gap is more stable and low chemical reactive. Thus, the value of energy gap is the most important indicator of the stability of molecules. The respective calculated HOMO and LUMO energies are -5.48 eV and 0.10 eV. The value of was found to be 5.58 eV. In addition, Huq in 2008 observed the HOMO-LUMO energy gap zoledronic acid and found it to be 6.14 eV at B3LYP/6-31G* [18]. This indicates that tenofovir has high chemically reactivity and low stability than zoledronic acid.

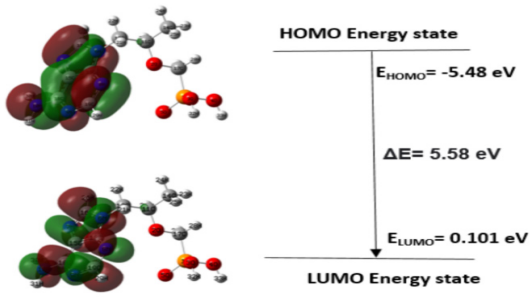

Figure 3: HOMO-LUMO plots of Tenofovir.

Figure 2: HOMO-LUMO surface mapping of tenofovir.

3.3 Molecular Electrostatic Potential (MEP) Surface

The charge distributions in molecules are represented in three dimensions by the MEP surface which infers the chemical reactive sites. The polar nature of the tenofovir is indicated by its dipole moment of 6.94 Debye. The presence of reactive sites in the subject molecule for electrophilic and nucleophilic assault was predicted using the MEP method. MEP contour surface of the title compound is shown in Figure 3. The electron concentrations at the MEP surface are indicated by different colors and increase in the order of Red > Orange > Yellow > Green > Blue [17,18].

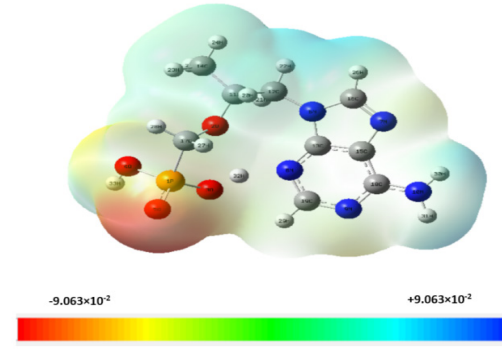

Figure 4: Molecular electrostatic potential (MEP) surface map of Tenofovir

Figure 3: Molecular electrostatic potential surface mapping of tenofovir.

The color representation of MEP for the investigated molecule is in the range (-9.063 to +9.063) 10^{-2} a.u. The most negative potential is seen across P1-O5 and O4-H and these are the nucleophiles regions. Similarly the most positive potential is seen across amine group.

3.4 Mulliken Population Analysis

Electronegative atoms such as nitrogen, oxygen, and carbon, along with several oxygen and nitrogen atoms like: O2, O3,

O4, O5, N7, N8, N9 and, N10 exhibit partial negative charges. On the other hand, all hydrogen atoms and some carbon atoms along with phosphorus, including C11, C15, C18, and C19, develop partial positive charges. Notably, N6 shows the most pronounced negative charge (-0.75 e), while P1 exhibits the highest positive charge (1.5 e). Despite being attached to an electronegative oxygen atom, N6 develops a partial negative charge due to the resonance effect of the benzene ring, which causes it to exhibit electron-withdrawing properties. In contrast, P1, is connected to oxygen atoms. This configuration causes P1 to display an electron-donating effect towards the oxygen atoms, leading to a partial positive charge. In tenofovir, the distribution of partial negative and partial positive charges is balanced across an equal number of atoms, highlighting the intricate electronic interactions within the molecule and underscoring its potential in drug design and molecular modification. The partial distribution of charges on the different atoms of tenofovir from Mullikan population analysis is depicted in Figure 4.

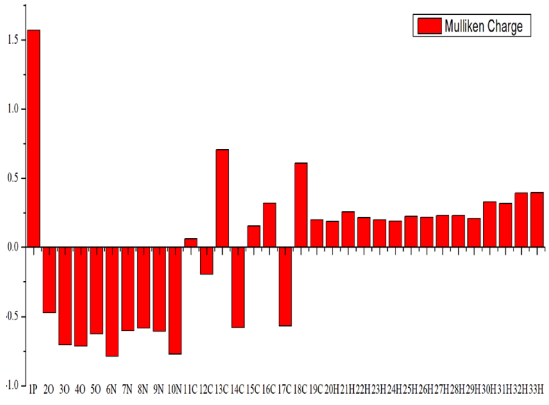

Figure 4: Mulliken charge associated with each atoms of tenofovir using B3LYP/3-21G.

3.5 Global Reactivity Descriptors

The calculated HOMO energy (E_H), LUMO energy (E_L), and their energy gap and the important parameters such as HOMO-LUMO energies, global softness, global hardness, electronegativity, global electrophilicity index and chemical potential are evaluated for the title molecule are listed in Table 1. The HOMO-LUMO energy gap of the examined molecule is obtained as 5.58 eV. Various reactivity descriptors are calculated with the help of Koopman's theorem [19,20]. The electronegativity (χ) value is 2.68 eV. The global hardness (η) is -2.29 eV and the global softness (S) is -0.21 eV^{-1}. These values are used to indicate the softness in comparison with other molecules. The global electrophilicity index (ω) is -1.57 eV which tells that the tenofovir shows electrophilic nature. The chemical potential (μ) value of a molecule is -2.68 eV.

Table 1: HOMO energy (E_H), LUMO energy (E_L), energy gap (E_L-E_H), electronegativity (χ), chemical potential (μ), global hardness (η), global softness (S), and global electrophilicity index (ω) for tenofovir.

E_H (eV)	-5.48
E_L (eV)	0.10
E_L-E_H (eV)	5.58
χ (eV)	2.68
μ(eV)	-2.68
η (eV)	-2.29
S (eV^{-1})	-0.21
ω (eV)	-1.57

3.6 Local reactivity descriptors

The Fukui function (FF) was used to determine the reactivity of each atom in the molecule. The atom with the highest FF value is more likely to participate in the reaction than other atoms in molecule [21]. The FF (f_k^+,f_k^-,f_k^0), local softness (S_k^+,S_k^-,S_k^0), and local electrophilicity indices (ω_k^+,ω_k^-,ω_k^0) determine the reactivity of each atom in the anion, cation, and neutral states. To get these characteristics, partial charges on each atom were estimated using Hirshfeld population analysis and Fukui functions [22].

$f_k^+ = [q_k(N + 1) - q_k(N)]$ for nucleophilic attack

$f_k^- = [q_k(N) - q_k(N - 1)]$ for electrophilic attack

$f_k^0 = [q_k(N + 1) - q_k(N - 1)]$ for radical attack

where q_k is the atomic charge at the k^{th} atomic site in the neutral (N), anionic (N+1) or cationic (N-1) state of the molecule. The local reactivity descriptor of tenofovir for selected atoms has been calculated, which inferred that the sites O2, O3, O4, O5, N6, N8, N9, N10, C13, C15, C17, H20, H24, H28, H30, and H31 are close to the nucleophilic center, whereas, the atoms P1, N7, C11, C12, C14, C16, C18, C19, H21,H22, H23, H25, H26, H27, H29, H32, and H33 are prone to electrophilic center. This also justified by Mulliken partial charge analysis. The highest value of f_k^+ is calculated across N10 (~0.1787) and the highest value of f_k^- (0.1467) is identified across C16 and these atoms are prone to eletrophilic and nucleophilic attack in the tenofovir, respectively.

Natural Bond Orbital (NBO) Analysis

NBO analysis has been performed via second-order perturbation theory to reveal all the possible interactions between filled donor Lewis type and virtual acceptor Lewis type NBOs orbital and their stabilization energy E(2) have been analyzed [23]. The interaction energy E(i,j) between i (donor) and j (acceptor) NBOs is numerically described which gives the stabilization energy among bonding and anti-bonding interaction. It is mathematically obtained from the off-diagonal Fock matrix element [23].

$E^{(2)} = E(i, j) = qi$

Where, E_i is referred to as the donor orbital occupancy and Ej are the respective energy of acceptor orbitals and Fij are the off-diagonal Fock- matrix elements. The larger value of (2) implies the more intensive donor-acceptor interactions. The different types of donor-acceptor interactions and their equilibrium energies are determined by second-order perturbation analysis of the Fock matrix of tenofovir and are tabulated in Table 2.

Table 2: Second-order perturbation theory analysis of Fock matrix in NBO basis of tenofovir.

Donor NBO (i)	ED(i)/e	Acceptor NBO(j)	ED(j)/e	E(2) (kcal/mol)	[E(j)-E(i)] (a.u.)	F(i,j) (a.u.)
π(N6-C13)	1.83301	LP(1)C15	1.12112	14.64	0.23	0.071
π(N6-C13)	1.83301	π*(N7-C16)	0.34923	18.18	0.34	0.092
σ(N7-C16)	1.98443	σ*(C15-C18)	0.03906	5.54	1.44	0.080
π(N7-C16)	1.88678	LP(1)C15	1.12112	34.86	0.19	0.102
σ(N8-C19)	1.98511	σ*(N6-C13)	0.04915	7.83	1.27	0.090
π(N8-C19)	1.77683	π*(N6-C13)	0.72852	42.90	0.24	0.104
π(N8-C19)	1.77683	π*(N9-C18)	0.46454	8.70	0.28	0.047
π(N9-C18)	1.69963	LP(1)C15	1.12112	27.37	0.16	0.092
π(N9-C18)	1.69963	π*(N8-C19)	0.37349	35.95	0.29	0.092
σ(C13-C15)	1.96977	σ*(C15-C18)	0.03906	5.23	1.31	0.074
LP(2) O2	1.91655	σ*(C11-C14)	0.02513	5.94	0.63	0.055
LP(2) O2	1.91655	σ*(C11-H20)	0.03368	6.27	0.70	0.060
LP(2) O2	1.91655	σ*(C17-H27)	0.02817	6.13	0.69	0.059
LP(2) O2	1.91655	σ*(C17-H28)	0.03242	7.40	0.68	0.064
LP2(O3)	1.90846	σ*(P1-O4)	0.27816	17.42	0.43	0.081
LP(2) O3	1.91029	σ*(P1-O5)	0.12205	9.79	0.55	0.066
LP(2) O4	1.91029	σ*(P1-O3)	0.27000	16.86	0.44	0.081
LP(2) O4	1.76172	σ*(P1-O5)	0.12205	9.83	0.56	0.067
LP(2) O5	1.76172	σ*(P1-O3)	0.27000	21.61	0.34	0.077
LP(2) O5	1.76172	σ*(P1-O4)	0.27816	6.78	0.34	0.043
LP(2) O5	1.76172	σ*(P1-C17)	0.16227	25.28	0.41	0.092
LP(3) O5	1.73609	σ*(P1-O3)	0.27000	27.44	0.33	0.086
LP(3) O5	1.73609	σ*(P1-O4)	0.27816	42.80	0.33	0.107
LP(1) N7	1.92554	σ*(N6-C16)	0.03757	7.30	0.77	0.067
LP(1) N7	1.92554	σ*(C13-C15)	0.04543	5.23	0.92	0.062
LP(1) N8	1.90013	σ*(N9-C19)	0.03000	10.75	0.81	0.085
LP(1) N8	1.90498	σ*(C13-C15)	0.04543	8.32	0.91	0.079
LP(1) N9	1.90013	σ*(N8-C19)	0.03212	11.76	0.80	0.088
LP(1) N9	1.90013	σ*(C15-C18)	0.03906	7.40	0.90	0.074
LP(1) N10	1.75030	π*(N9-C18)	0.46452	52.96	0.23	0.105
LP(1) C15	1.12112	π*(N6-C13)	0.72852	246.24	0.07	0.125
LP(1) C15	1.12112	π*(N7-C16)	0.34923	60.46	0.11	0.086
LP(1) C15	1.12112	π*(N9-C18)	0.46454	114.43	0.12	0.117

The interaction of (N8-C19) → $\pi*$ (C6-C13) produces resonance in the molecule, leading to stabilization energy of 42.90 kcal/mol. A very strong interaction has been identified

between the loan pair LP(1)C15 → $\pi*$ (N6-C13) which stabilizes the molecule with stabilization energy 246.24 kcal/mol. The loan pair LP(1) N7 participates in charge transfer from LP(1)N7 → $\sigma*$ (N6-C16)/$\sigma*$ (C13-C15) with energies of 7.30/5.23 kcal/mol. The interactions LP(2)O3 → $\sigma*$ (P1-O4) lead to a stabilization energy of 17.42 kcal/mol.

3.8 Vibrational Analysis

The title molecule has 33 atoms so it has 93 (3N - 6) modes of vibration including stretching and bending. The graph of FT-IR absorbance and Raman the intensity of the investigated molecule with wavenumber is plotted. The plot is presented in Figures 5 and 6 respectively.

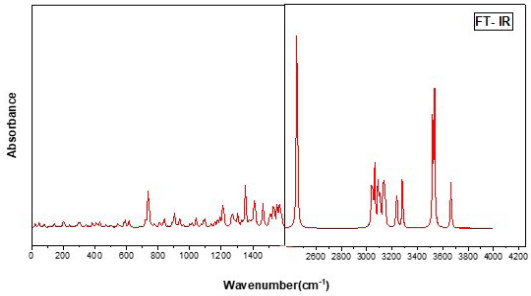

Figure 5: FT-IR spectroscopy of tenofovir.

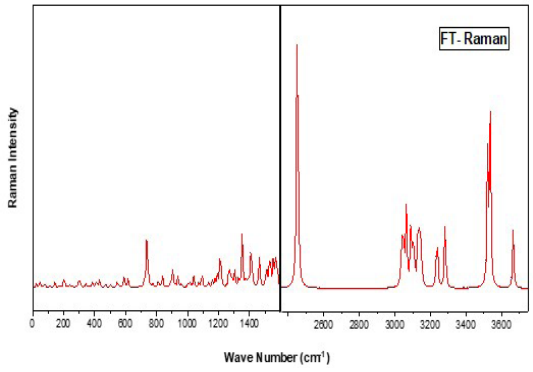

Figure 6: Graph of FT-Raman spectroscopy of tenofovir.

3.8.1 Vibration of CH_2 group

The wagging vibration range of the CH_2 group is (1368 – 1300) cm^{-1} [24]. The out plane bending frequency is calculated at 1330.11 cm^{-1}. The CH_2 symmetric stretching and asymmetric stretching frequencies are observed at 3044.66 and 3106.56 cm^{-1} respectively. Both are found in the Raman band.

3.8.2 Vibration of the hydroxyl group

The stretching vibration of the (-OH) group is in the range of (3100 – 3690) cm^{-1} [25]. In this research, we have observed the hydroxyl stretching at 3521.85 cm^{-1}. Similarly, the bending was observed at 48.67 cm^{-1}. Both results are observed in IR band.

3.8.3 Vibration of phosphonate group

The bending of the phosphonate group was observed in the range (314.73 - 509.56) cm^{-1} [24,25]. In this region, the IR band was active which means a vibration results in a change in the molecular dipole moment. The stretching of the phosphonate group is in the range of (281.11 - 411.64) cm^{-1}

4. Conclusions

The minimum energy of tenofovir was measured to be -7.91×10^5 kcal/mol. The least value of bond length ~ 0.99 Å was calculated across O4-H33 and highest value of bond length ~ 1.87 Å was calculated across P1-C17. Moreover, the maximum value of bond angle is calculated as 131.16 ° and minimum value is 96.48 ° across N6-C13-N8 and O4-P1-C17 respectively. These findings are due to inter molecular hydrogen bonding with surrounding

species. The HOMO and LUMO energies has been examined as - 5.48 and 0.101 eV respectively. The value of has been obtained as 5.58 eV. The global reactivity parameters such as: electronegativity (χ), chemical potential (μ), global hardness (η), and global electrophilicity index (ω) have been obtained as 2.68, -2.68, -2.29, and -1.57 eV respectively. The global softness (S) has been found to be -0.21eV^{-1}. The phosphonate group which acts as a nucleophilic center and amine group acts as electrophilic center in the MEP surface analysis. The value of f_k^+ across N10 is determined as ~0.1787 and the value of f_k^- across C16 is calculated as ~ 0.1467. The highest value of FF across N10 and C16 predict that former atom is more nuleophilic sites and latter one more electrophilic site. From spectroscopic analysis, the respective wave number for symmetric and asymmetric stretching of CH_2 has been calculated at 3044.66 and 3106.56 cm^{-1} but the out plane bending is calculated at 1330.11 cm^{-1}.

Acknowledgment
We are grateful to Prof. Dr. Poonam Tandon, Lucknow University for providing the software facility.

Author contribution
M. K. Chaudhary: Drafting, and Data analysis; S. Poudel: Manuscript writing and reviewing; J. Shahi: Analysis, and drafting; P. R. Sharma: Conceptualization of research activity.

Declarations Conflict of interest
The authors declare no competing interests

References

[1] National Center for Biotechnology Information. PubChem Compound Summary for CID 464205, Tenofovir. Retrieved November 26, (2024) from https://pubchem.ncbi.nlm.nih.gov/compound/Tenofovir.

[2] K.F. Murray, L. Szenborn, J. Wysocki, S. Rossi, A.C. Corsa, P. Dinh, J. McHutchison, P.S. Pang, L.M. Luminos, M. Pawlowska, and J. Mizerski,. Randomized, placebo-controlled trial of tenofovir disoproxil fumarate in adolescents with chronic hepatitis B. Hepatology, 56(6), pp.2018-2026 (2012).

[3] R.T. Schooley, P. Ruane, R.A. Myers, G. Beall, H. Lampiris, D. Berger, S.S. Chen, M.D. Miller, E. Isaacson, and A.K. Cheng. Tenofovir DF in antiretroviral-experienced patients: results from a 48-week, randomized, double-blind study. Aids, 16(9), pp.1257-1263 (2002).

[4] M.N.Arimilli,C.U.Kim,J.Dougherty, A. Mulato, R. Oliyai, J.P. Shaw, K.C. Cundy, and N. Bischofberger. Synthesis, in vitro biological evaluation and oral bioavailability of 9-[2-(phosphonomethoxy) propyl] adenine (PMPA) prodrugs. Antiviral Chemistry and Chemotherapy, 8(6), pp.557-564 (1997).

[5] L. Naesens, N. Bischofberger, P. Augustijns, P. Annaert, G. Van den Mooter, M.N. Arimilli, C.U.Kim, and E. De Clercq. Antiretroviral efficacy and pharmacokinetics of oral bis (isopropyloxycarbonyloxymethyl) 9-(2-phosphonylmethoxypropyl)

adenine in mice. Antimicrobial agents and chemotherapy, 42(7), pp.1568-1573 (1998).

[6] K. Squires, A.L. Pozniak, G. Pierone Jr, C.R. Steinhart, D. Berger, N.C. Bellos, S.L. Becker, M. Wulfsohn, M.D. Miller, J.J. Toole, and D.F. Coakley. Tenofovir disoproxil fumarate in nucleoside-resistant HIV-1 infection: a randomized trial. Annals of internal medicine, 139(5_Part_1), pp.313-320 (2003).

[7] M.J. Frisch, G.W. Trucks, H.B. Schlegel, G.E. Scuseria, M.A. Robb, J.R. Cheeseman, G. Scalmani, V. Barone, B. Mennucci, G.A. Petersson, and H. Nakatsuji. Uranyl extraction by N, N-dialkylamide ligands studied by static and dynamic DFT simulations. In Gaussian 09. Gaussian Inc Wallingford (2009).

[8] P. Hohenberg, and W. Kohn. Inhomogeneous electron gas. Physical review, 136(3B), pp.B864 (1964).

[9] A.D. Becke. Density-functional thermochemistry. I. The effect of the exchange-only gradient correction. The Journal of chemical physics, 96(3), pp.2155-2160 (1992).

[10] C. Lee, W. Yang, and R.G. Parr. Development of the Colle-Salvetti correlation-energy formula into a functional of the electron density. Physical review B, 37(2), pp.785 (1998).

[11] T.H. Dunning Jr . Gaussian basis sets for use in correlated molecular calculations. I. The atoms boron through neon and hydrogen. The Journal of chemical physics, 90(2), pp.1007-1023(1989).

[12] D.E. Woon, and T.H Dunning Jr. Gaussian basis sets for use in correlated molecular calculations. V. Core-valence basis sets for boron through neon. The Journal of chemical physics, 103(11), pp.4572-4585 (1995).

[13] A. Petersson, A. Bennett, T.G. Tensfeldt, M.A. Al-Laham, W.A. Shirley, and J. Mantzaris. A complete basis set model chemistry. I. The total energies of closed-shell atoms and hydrides of the first-row elements. The Journal of chemical physics, 89(4), pp.2193-2218 (1988).

[14] A. Frisch, A. Nielson, and A. Holder. Gauss view user manual. Pittsburgh, PA: Gaussian (2005).

[15] T. Chaudhary, M.K. Chaudhary, B.D. Joshi, A Theoretical Study on Charge Transfer and Hyperpolarizability of (S)-2-amino-3-(3, 4-dihydroxyphenyl)-2-methyl-propanoic Acid, JNPS, 8(1) (2022) 16-21. ISSN: 2392-473X (Print), 2738-9537 (Online)

[16] A. K. Srivastava, A.K. Pandey, S. Jain, and N. Misra. FT-IR spectroscopy, intra-molecular C–H⋯ O interactions, HOMO, LUMO, MESP analysis and biological activity of two natural products, triclisine and rufescine: DFT and QTAIM approaches. Spectrochimica Acta Part A: Molecular and Biomolecular Spectroscopy, 136, pp.682-689 (2015).

[17] F. Huq. Molecular Modelling Analyses of Metabolism of Zoledronic Acid, Pamidronate and Clodronate.

[18] N. Gonohe, H. Abe, N. Mikami, and M. Ito. Two-color photoionization of van der Waals complexes of fluorobenzene and hydrogen-bonded complexes of phenol in supersonic jets. The Journal of Physical Chemistry, 89(17), pp.3642-3648 (1985).

[19] M.K. Chaudhary, P. Prajapati, and B. D. Joshi. "Quantum Chemical Calculation and DFT Study of Sitagliptin: Insight from Computational Evaluation and Docking Approach." Journal of Nepal Physical Society 6, no. 1: pp.73-83(2020).

[20] M. Changxing, X. Guixiang, and Z. Lifeng. The Cauchy problem of the Hartree equation. Journal of Partial Differential Equations, 21(1), p.22 (2008).

[21] J.L.Gázquez. Perspectives on the density functional theory of chemical reactivity. Journal of the Mexican Chemical Society, 52(1), pp.3-10 (2008).

[22] J.B. Ott, J. Boerio-Goates, and D.E. Beasley. Chemical thermodynamics: principles and applications. Applied Mechanics Reviews, 54(6), pp.B110-B110 (2001).

[23] H.D. Lutz, W. Eckers, and H. Haeuseler. OH stretching frequencies of solid hydroxides and of free OH− ions. Journal of Molecular Structure, 80, pp.221-224 (1982).

[24] N.B. Colthup, L.H. Daly, S.E. Wiberley, Introduction to Infrared and Raman Spectroscopy, Academic Press, New York, (1990).

[25] G. Varsanyi, Assignments for Vibrational Spectra of Seven Hundred Benzene Derivatives, vols. 1 and 2, Academia Kiado, Budapest (1973).